Green Chemistry

PAPER

View Article Online
View Journal | View Issue

Cite this: *Green Chem.*, 2025, **27**, 2554

Synthesis and chemical recycling of biobased poly(acetal-ester)s with a non-cyclic acetal unit†

Niklas Warlin, [a,b] Sathiyaraj Subramaniyan,[a] Maria Nelly Garcia Gonzalez, [c] Rafael N. L. de Menezes, [a] Smita V. Mankar,[a,d] Nitin G. Valsange,[a] Nicola Rehnberg,[a,e] Patric Jannasch *[a] and Baozhong Zhang *[a]

Received 12th November 2024,
Accepted 31st January 2025

DOI: 10.1039/d4gc05778c

rsc.li/greenchem

There is a high demand to design and develop recyclable biobased polymers using eco-friendly synthetic approaches. In this work, we present the facile synthesis of two dicarboxylate monomers with a central non-cyclic acetal unit (dimethyl 4,4′-(methylenebis(oxy))dibenzoate and dimethyl 4,4′-(methylenebis(oxy))bis(3-methoxybenzoate)), using potentially bio-sourced methyl paraben and methyl vanillate. The synthetic parameters were evaluated by a cradle to gate life cycle greenhouse gas emissions aiming to understand the environmental impacts. The two monomers were subjected to melt polycondensation with three linear aliphatic diols (ethylene glycol, 1,4-butanediol, and 1,6-hexanediol) with varied lengths and flexibility to yield six polyesters with molecular weights (M_n) ranging from 10–19 kDa, tunable glass transition (T_g ~ 41–83 °C), and relatively high thermal stability. Most of the obtained biobased polyesters were amorphous, except for the polymer derived from butanediol and methyl paraben, which showed slow crystallization according to differential scanning calorimetry results. We discovered that the non-cyclic acetal bonds in the poly(acetal-ester)s could be selectively hydrolyzed under mild temperature (70 °C) by varying the acid concentration, offering a potential strategy for chemical recycling.

Green foundation

1. Biobased polyesters containing non-cyclic acetal units were designed and synthesized, which showed decent thermal stability and tunable glass transition temperatures, and they could be conveniently depolymerized under mild acidic conditions to yield monomers that are suitable for repolymerization.
2. The molecular design towards biobased polyesters with chemical recyclability based on non-cyclic acetal structures was demonstrated. The environmental impacts of the synthetic factors were preliminarily understood by LCA.
3. In the future, various possibilities of repolymerization of the monomers obtained from acidic depolymerization of the new polyesters with non-cyclic acetals could be investigated in detail, which is expected to provide insights into closed-loop recycling or upcycling.

Introduction

Conventional plastics have received growing environmental concerns, such as plastics littering, greenhouse gas emissions, and global warming.[1] The transition toward sustainable biobased plastics has been considered a solution to some of these challenges.[2–5] However, biobased polymers have been frequently criticized for imposing challenges in the current recycling process.[6,7] Today, most polymers are recycled by thermomechanical processes (*i.e.*, mechanical recycling), which requires perfect sorting and separation of different types of polymers.[8,9] Any new polymer (even biobased ones) may further complicate the sorting of mixed plastic waste and thus hinder mechanical recycling.[10] Therefore, alternative recycling

[a]*Centre for Analysis and Synthesis, Department of Chemistry, Lund University, P.O. Box 124, SE-22100 Lund, Sweden.*
E-mail: baozhong.zhang@chem.lu.se, patric.jannasch@chem.lu.se
[b]*Department of Chemistry, Stanford University, Stanford, California 94305-5080, USA*
[c]*Environmental and Energy Systems Studies, Department of Technology and Society, Lund University, PO Box 118, SE-221 00 Lund, Sweden*
[d]*Department of Chemical Engineering, Massachusetts Institute of Technology, 77 Massachusetts Avenue, Cambridge, Massachusetts 02139, USA*
[e]*Bona Sweden AB, R&D, Box 210 74, SE-200 21 Malmö, Sweden*
† Electronic supplementary information (ESI) available. See DOI: https://doi.org/10.1039/d4gc05778c

methods based on chemical or biological processes have been under intensive development,[11–18] aiming to enhance the recyclability of new biobased polymers. In this context, bio-based polymers with acetal units (namely polyacetals) have received growing attention because acetal bonds can be conveniently cleaved under acidic conditions, which may facilitate chemical recycling.[19–24]

The outcome of acidic hydrolysis of polyacetals can be different if their backbones contain other acid labile functional groups (*e.g.*, esters, amides, urethanes, *etc.*). For instance, our group has recently synthesized lignin-based poly(acetal-ester)s that can be selectively depolymerized by acetal hydrolysis, while leaving the ester bonds completely intact.[19] This enabled energy-efficient short-loop chemical recycling *via* the formation and repolymerization of telechelic polymers. Interestingly, the ester bonds in a different xylose-based poly(acetal-ester) could be selectively hydrolyzed under acidic conditions, leaving the cyclic acetal bonds intact.[25] Other cyclic acetal units have also been used for the design and synthesis of biobased chemically-recyclable polyacetals, which yielded different building blocks upon acidic hydrolysis.[15,19,26] In addition, noncyclic acetals have been investigated in the development of drug delivery vehicles[27–30] and crosslinked thermoset resins[31–33] which are generally easier to hydrolyze compared to cyclic acetals.[23,34] Surprisingly, noncyclic acetals have received little attention in the development of chemical recyclable thermoplastic polymers, and the structure–property relationship concerning their acidic hydrolysis remains largely unknown.

Another frequently encountered criticism of bioplastics is whether they are truly eco-friendly simply because they are made from renewable carbon.[35] Although the use of renewable biomass sources can be generally perceived as sustainable, the production of raw materials and polymers often involves many different parameters such high temperature, and the use of solvents and catalysts. The full environmental impacts of bioplastic synthesis can thus be difficult to predict. As such, preliminary life cycle assessments (LCA) have recently started gaining popularity in the development of new bioplastics. For instance, the design and synthesis of plant oil-based acrylic monomers were optimized to minimize their environmental impacts according to LCA.[36] In another approach, a prospective LCA was used to assess the chemical and biocatalytic synthesis of a lactone-based monomer.[37] In our own efforts to develop new sugar- or lignin-based polymers, a preliminary LCA was used to confirm the low greenhouse gas (GHG) emissions of diol – and dicarboxylate monomers containing spirocyclic acetal structures.[15,22,38,39] However, the use of LCA in the synthesis of new bioplastics is still rare, presumably due to the lack of LCA data for most new molecules.

Herein, we report the molecular design and synthesis of two new dicarboxylate monomers with a non-cyclic formaldehyde-based acetal unit using the potentially bio-based monomeric building blocks methyl vanillate and methyl paraben (Scheme 1).[40,41] Various synthetic parameters were optimized according to their preliminary GHG emissions. The monomers were reacted with linear aliphatic diols to produce two series of poly(acetal-ester)s, of which the molecular, thermal characteristics and chemical recyclability under acidic conditions were preliminarily investigated. The impact of methoxy groups on the acidic stability of the obtained polymers was also investigated.

Experimental

Materials

Potassium carbonate (K_2CO_3, 99%), dibutyltinoxide (DBTO, 98%), ethylene glycol (99%), mesitylene (98%), $CDCl_3$ (99.8% atom D, 1% TMS), 1,6-hexanediol (97%), dimethylsulfoxide (DMSO, 99.9%), DMSO-d_6 (99.9% atom D), KI (99%), methyl vanillate (99%), methyl paraben (99%), and dibromomethane (99%) were purchased from Sigma Aldrich. Acetone (99.8%) was purchased from Acros. $NaHCO_3$ (99.7%) and 2-propanol (99.8%) were purchased from Merck. 1,4-Butanediol (99%) was purchased from Riedel de haen. Xylenes was purchased from Scharlau. NaOH and chloroform (99.8%) were purchased from Fischer. Methanol, dichloromethane (DCM), *tert*-butanol (*t*-BuOH), and acetonitrile (ACN) were purchased from VWR chemicals. All solvents were of analytical grade or higher, and all reagents and chemicals were used without further purification.

Analytical methods

^{1}H and ^{13}C NMR measurements were performed on a Bruker DR X400 spectrometer at 400.13 MHz and 100.61 MHz, respectively. Chemical shifts were reported as δ values (ppm). HRMS (high-resolution mass spectrometry) was performed on a Micromass QTOF mass spectrometer (ESI). Size exclusion chromatography (SEC) measurements for the polyesters were carried out using Malvern Viscotek TDAmax instrument with a 2 × PL-Gel Mix-B LS column set (2 × 30 cm) equipped with OmniSEC triple detectors (refractive index, viscosity and light scattering) and chloroform as eluent at 35 °C at a flow rate of 1 mL min^{-1}. Calibration was performed with a narrow polystyrene standard M_p = 96 000 Da, $Đ$ = 1.03 (Polymer Laboratories Ltd, Agilent Technologies and Water Associates). Fourier transform infrared (FTIR) spectra were measured with an attenuated total reflection (ATR) setup using a Bruker Alpha II FT-IR spectrometer. TGA (thermogravimetric analysis) measurements were carried out on a TA instrument mode TGA Q500. The measurement was performed by heating from 50–600 °C with a heating rate of 10 °C min^{-1}. DSC (differential scanning calorimetry) measurements were performed on a DSC Q2000 analyzer from TA instruments. Data was recorded from −50 to 200 °C, and T_g was determined from the second heating cycle. Annealing was performed at 10 °C below the T_m observed in the first heating cycle. The synthesized polyesters were made into films of dimensions (17.5 × 5.5 × 1 mm) for dynamic mechanical analysis (DMA). DMA measurements were performed in a stretching mode using TA instruments Q800 analyzer. The measured samples were heated from 20 °C to 100 °C at a heating rate of 3 °C min^{-1} and frequency of 1 Hz with strain of 0.1%.

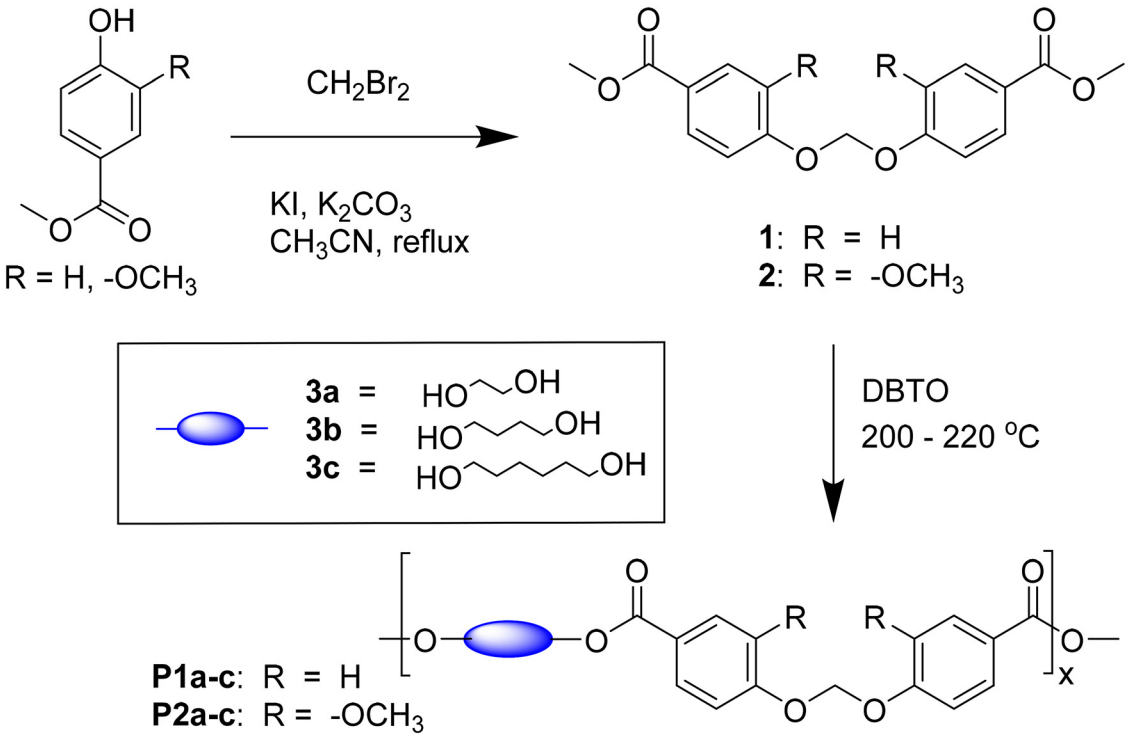

Scheme 1 Synthesis of dicarboxylate monomers **1** and **2** and their polymerization with three aliphatic diols **3a–c** to prepare polyesters **P1a–c** and **P2a–c** (a–c in the polymer names indicate the use of aliphatic diols **3a–c** for polymerizations, respectively).

Assessing global GHG emissions

The comparative analysis between Monomers **1** and **2** was performed following LCA methodology, which is standardized in the ISO 14040-14044 series by the International Organization of Standardization. The lab data was incorporated into the SimaPro LCA software, and the Ecoinvent database version 3.8. (allocation at the point of substitution (APOS) system model) was used as a background source. The foreground data was then evaluated. The functional unit was "kg of monomer". The system boundary was set up following a cradle-to-factory gate approach. At this early stage, the study was based on the IPCC 2021 method, which contains the Global Warming Potential (GWP100) climate change factors of IPCC with a timeframe of 100 years. The most important precursor emissions originating from this impact category are carbon dioxide (CO_2), nitrous oxide (N_2O), and methane (CH_4). The characterization factors needed to quantify how much impact the new monomers have in GHG emissions are taken from the IPCC 2021 method.

We assumed that the energy required to produce 1 kg of monomer was equal to the energy required to produce 1 kg of polyvinylchloride by emulsion polymerization at 70–90 °C. The energy required for heating the reaction was calculated according to eqn (1), ESI.† The energy costs and reagents were taken from the Ecoinvent database, version 3.8. The energy cost to produce the solvent was excluded. LCA data for dibromomethane was unavailable, so its analogous molecule dichloromethane was used for calculations. The LCA data on 4-hydroxybenzoic acid (4-HBA) based on cane sugar was taken from Krömer *et al.* (6.57 kg CO_2-eq per kg 4-HBA).[42] In this study, results are given in a range of 5.96–12.25 kg CO_2-eq per kg 4-HBA. These values depended on recycling of the biomass, the type of feedstock *etc*. Our choice was based on the scaled up base case for non-recycled biomass, and the intermediate value for the available feedstocks was taken as an average.[42] Transportation of the feedstock and solvents from one factory to the other for the monomer production was excluded.

The LCA data on lignin-derived vanillin was taken from Borregaard (0.7 kg CO_2-eq per kg DM).[43] To this value was added the estimated GHG emissions corresponding to the process of oxidizing vanillin to vanillic acid. Since LCA data for the exact oxidation of vanillin to vanillic acid is unavailable in the Sima Pro software, the GHG emissions for the oxidation of a similar molecule, toluene, into benzoic acid was used as an approximation (0.41 kg CO_2-eq per kg molecule). The total GHG emissions to produce vanillic acid were therefore estimated as 1.11 kg CO_2-eq per kg vanillic acid.

Monomer synthesis

To a 250 mL round bottom flask equipped with magnetic stirrer, dibromomethane (5.00 g, 0.0285 mol), methyl paraben (8.75 g, 0.0575 mol), potassium carbonate (8.74 g, 0.0632 mol) and potassium iodide (0.477 g, 0.0028 mol) were added. Afterwards, acetonitrile (100 mL) was added until the reagents were completely dissolved. The reaction was heated with reflux for 24 h, and then poured into cold water (1000 mL) to form a white precipitate. The precipitate was collected by vacuum filtration, washed with cold water (200 mL), and dried at 50 °C in vacuum oven to give monomer **1** as a white powder (8.0 g, 88%). ^{1}H NMR

(400.13 MHz, $CDCl_3$, δ, ppm): 8.00 (d, 4H, J = 8.93 Hz, Ar–H), 7.12 (d, 4H, J = 8.89 Hz, Ar–H), 5.81 (s, 2H, acetal CH_2), 3.88 (s, 6H, –$COOCH_3$) ^{13}C NMR (100.61 MHz, $CDCl_3$, δ, ppm): 166.56, 160.26, 131.64, 124.51, 115.75, 90.03, 51.99. HR-MS (ESI+, m/z): exact calculated for $[C_{17}H_{16}O_6 + Na]^+$: 339.0844 found 339.0845.

To a 250 mL round bottom flask equipped with a magnetic stirrer, dibromomethane (5.00 g, 0.0285 mol), methyl vanillate (10.5 g, 0.0575 mol), potassium carbonate (8.74 g, 0.0632 mol) and potassium iodide (0.477 g, 2.80 mmol) were added. Afterwards, acetonitrile (100 mL) was added until the reagents were completely dissolved. The reaction was heated with reflux for 24 h, and then poured into cold water (1000 mL) to form a white precipitate. The precipitate was collected by vacuum filtration, washed with cold water (200 mL), and dried at 50 °C in vacuum oven to give monomer **2** as a white powder (9.8 g, 91%). ^{1}H NMR (400.13 MHz, $CDCl_3$, δ, ppm): 7.63 (dd, 2H, J = 8.45 Hz, J = 1.98 Hz, Ar–H), 7.57 (d, 2H, J = 1.93 Hz, Ar–H), 7.28 (d, 2H, J = 8.49, Ar–H), 5.87 (s, 2H, acetal CH_2), 3.889 (s, 6H, –OCH_3), 3.886 (s, 6H, –$COOCH_3$). ^{13}C NMR (400.13 MHz, $CDCl_3$, δ, ppm): 166.65, 149.78, 149.57, 125.19, 123.26, 116.29, 112.93, 92.13, 56.06, 52.13. HR-MS (ESI+, m/z): exact calculated for $[C_{19}H_{20}O_8 + Na]^+$: 399.1052 found 399.1056.

Optimization of monomer synthesis

The synthetic procedure of reaction **F** was described as a typical example:

To a 25 mL round bottom flask equipped with magnetic stirrer, dibromomethane (171 mg, 0.980 mmol), methyl paraben (302 mg, 1.98 mmol), KI catalyst (34 mg, 0.2 mmol), and NaOH (88 mg, 2.2 mmol) were added. Afterwards, DMSO (5 mL) was added. The reaction was stirred at 56 °C for 24 hours after which a droplet was taken out, dried for 3 minutes under vacuum, and then analyzed by ^{1}H-NMR spectroscopy.

Polymer synthesis

The synthetic procedure of **P1b** was described as a typical example:

To a 25 mL round bottom flask equipped with mechanical stirrer, 1,4-butanediol (0.860 g, 9.54 mmol), DBTO (20 mg, 0.080 mmol), monomer **1** (2.00 g, 6.32 mmol) and 2 mL of xylenes were added. The reaction mixture was heated to 200 °C and stirred under nitrogen for 4 h. Afterwards, the temperature was increased to 220 °C with mesitylene (10 mL) added. A faster nitrogen flow was applied for 12 h to facilitate removal of the diol. Afterwards, the polymer was dissolved in chloroform and precipitated into methanol to give the polymer (**P1b**) as a white solid (1.90 g, 88%). ^{1}H NMR (400.13 MHz, $CDCl_3$, δ, ppm): 8.00 (d, 4 H, J = 8.92 Hz, Ar–H), 7.11 (d, 4 H, J = 8.91 Hz, Ar–H), 5.80 (s, 2 H, acetal CH_2), 4.35 (s, 4 H, O–CH_2–), 1.91 (s, 4 H, –CH_2–). ^{13}C NMR (100.61 MHz, $CDCl_3$, δ, ppm): 166.02, 160.26, 131.63, 124.61, 115.77, 90.02, 64.34, 25.58.

Chemical recycling

Acid hydrolysis of **P1a** was described as a typical example:

P1a (158 mg) powder was added to a 25 mL round bottom flask equipped with a magnetic stirrer. HCl (12 M, 15 mL) was added, and the reaction was stirred at 70 °C for 24 h. Afterwards, the solution was diluted with water (30 mL), and K_2CO_3 (9.16 g) was added until pH ≈ 1. Afterward, the slurry was filtered to give a solid as the main crude product (107 mg), which was the hydrolyzed bis-phenol structure. The aqueous phase was extracted with DCM (3 × 50 mL) and the combined organic phase was concentrated *in vacuo* to give another crude solid (3.5 mg), which was a mixture of small molecules formed by hydrolysis of the ester bonds in the polymer.

Ester hydrolysis

A typical example is described below.

Methyl vanillate (180 mg) was added to a 40 mL vial equipped with a magnetic stirrer. HCl (12 M, 5 mL) was added to the vial and the reaction was stirred at 70 °C for 1 h. Afterwards, the solution was diluted with water (10 mL), and K_2CO_3 (3.0 g) was added until pH ≈ 1. After this, the slurry was filtered to give a solid as the first crude product consisting primarily of methyl vanillate and vanillic acid (35.7 mg). The aqueous phase was extracted with DCM (3 × 15 mL) and the combined organic phase was concentrated *in vacuo* to give another crude solid consisting of methyl vanillate and vanillic acid (89.8 mg). For detailed calculations of the methyl vanillate content please see the ESI.†

Results and discussion

Synthesis and environmental analysis of monomers

The dicarboxylate ester Monomers **1** and **2** were synthesized by a straightforward S_N2 reaction of methyl vanillate or methyl paraben using dibromomethane according to a modified procedure from a patent (Scheme 1).[44] A mild base (K_2CO_3) was used to enhance the nucleophilicity of the phenol groups, and potassium iodide (KI) was used as catalyst. The reaction was completed in 24 h, which afforded Monomer **1** and **2** in good yields (88–91%) after a straightforward purification by precipitation in water. The monomers were unambiguously characterized by NMR, as shown in Fig. S1–8.†

The key reaction parameters influencing GHG emissions and conversion were evaluated for the synthesis of Monomer **1** from an environmental impact perspective. The Global Warming Potential (GWP), an index measuring the infrared thermal radiation absorption of a greenhouse gas over a given time frame, was calculated for various conditions. These included different solvents (ACN, acetone, DMSO, and *t*-BuOH), bases (NaOH and K_2CO_3), and reaction temperatures (20 °C to 82 °C), as detailed in Table S2 (ESI†). In general, the lowest GWP values coincided with the highest conversions, as this resulted in minimal waste of the reagents. Specifically, the optimal conditions were achieved using DMSO as the solvent, NaOH as the base, and a reaction temperature of 56 °C–82 °C. Similar GWP and yields were observed when the reaction was performed in ACN at 82 °C with NaOH as the base. Detailed results for all tested conditions and the individual impacts of each parameter on the GWP are provided in the ESI.†

Polyester synthesis and characterization

The two monomers (**1**,**2**) were polymerized by melt polycondensation with three linear aliphatic diols **3a–c** with varied lengths, yielding two series of polyesters (**P1a–c** and **P2a–c**, Scheme 1) with moderately high molecular weights (10.2–18.8 kDa) according to SEC results (Table 1 and Fig. S9–14†). Excess diol (1.5 eq.) was used to compensate for losses due to evaporation during the polycondensations.

Table 1 Summary of the properties for the monomers and polyesters[a]

Structure	Sample	M_n (kDa)	M_w (kDa)	$Đ$	T_g (°C)	T_5 (°C)	T_d (°C)	CY (%)
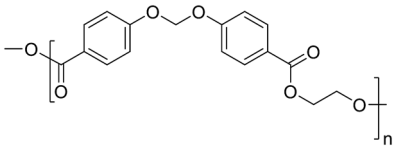	**P1a**	14.7	24.1	1.64	79	359	385	23
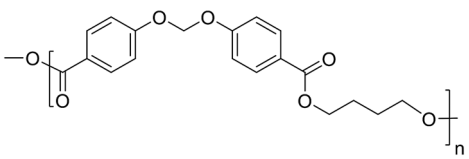	**P1b**	13.0	21.4	1.65	53	353	377	23
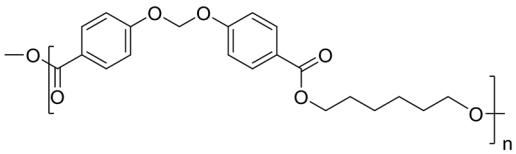	**P1c**	18.8	28.1	1.50	41	348	384	22
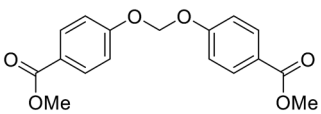	Monomer **1**	—	—	—	— 200	258	2	
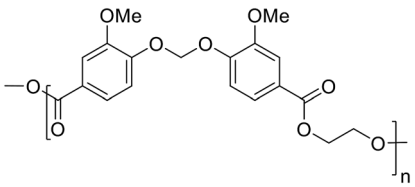	**P2a**	10.2	14.8	1.41	83	352	378	28
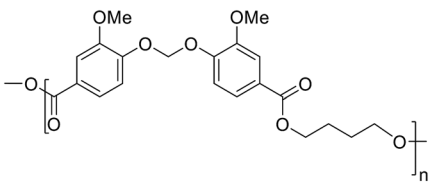	**P2b**	16.0	23.8	1.50	65	334	356	31
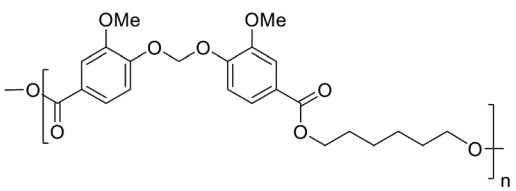	**P2c**	16.0	24.1	1.58	52	332	363	15
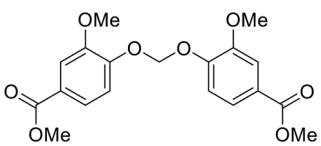	Monomer **2**	—	—	—	— 232	278	1	

[a] M_n and M_w was measured by SEC in chloroform. T_g was measured from the second heating curve in DSC. T_5, T_d and CY (char yield at 600 °C) were measured by TGA.

A small volume (2 mL) of xylene was added to reduce the viscosity and thus facilitate the polycondensations.[45–47] The reaction was initially performed at 200 °C under nitrogen to form oligomers by transesterification. After 4 h, the temperature was raised to 220 °C with a faster nitrogen flow to facilitate removal of the condensed diol and shift the reaction equilibrium towards higher molecular weight polymers. The reaction was completed after an additional 12 h, and the resulting crude was dissolved in chloroform and precipitated in methanol to yield the polyesters as white powders. The chemical structures of the polyesters were characterized using FTIR and ^{1}H NMR spectroscopy (Fig. S15–32, ESI†).

Thermal properties

The thermal stability of the polyesters was investigated by TGA (Fig. 1). All the polyesters exhibited an initial thermal decomposition temperature (T_5) above 330 °C, which is comparable to many other bio-based polyesters.[48,49] A single decomposition step was observed for all polymers (Fig. 1B), which could be due to the degradation of the ester bond by the typical beta hydrogen transfer mechanism.[50,51]

Polyesters **P1a–c** and **P2a–c** were further characterized by DSC measurements (Fig. 2). As shown in the second heating curves (Fig. 2A), most polyesters were fully amorphous without any melting endotherm. The only exception was **P1b**, which showed a small melting endotherm at ~150 °C. However, no corresponding crystallization exotherm was observed in its 1st cooling curve (Fig. 2B), which indicated a slow crystallization process. The T_g values of the polyesters ranged from 41 to 83 °C (Fig. 2A and Table 1), and decreased with an increased length of the diol, which was consistent with the increased backbone flexibility.[52,53] This T_g is within the range for many

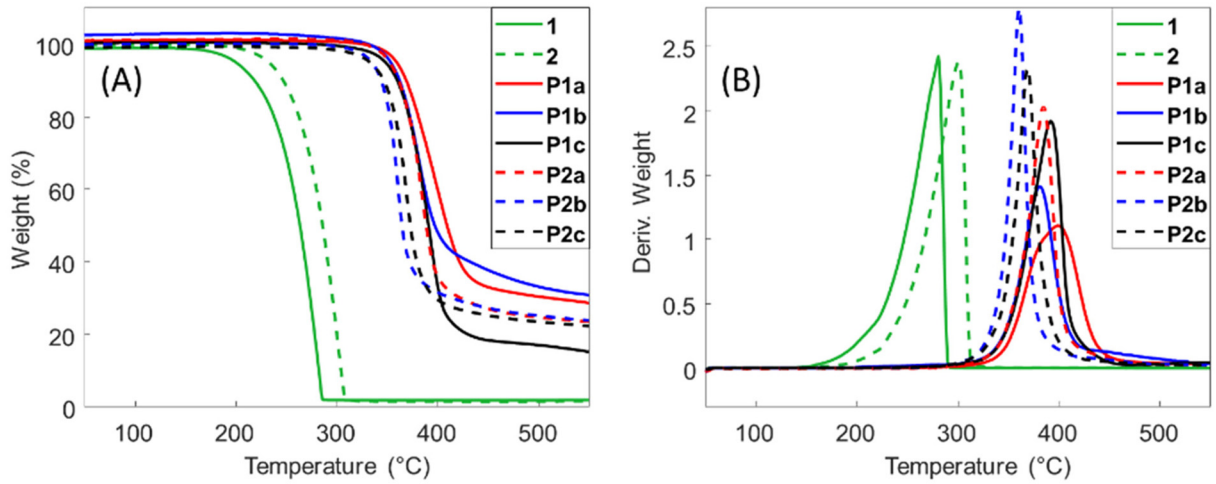

Fig. 1 Thermograms (A) and 1st derivative curves (B) of the monomers and polymers.

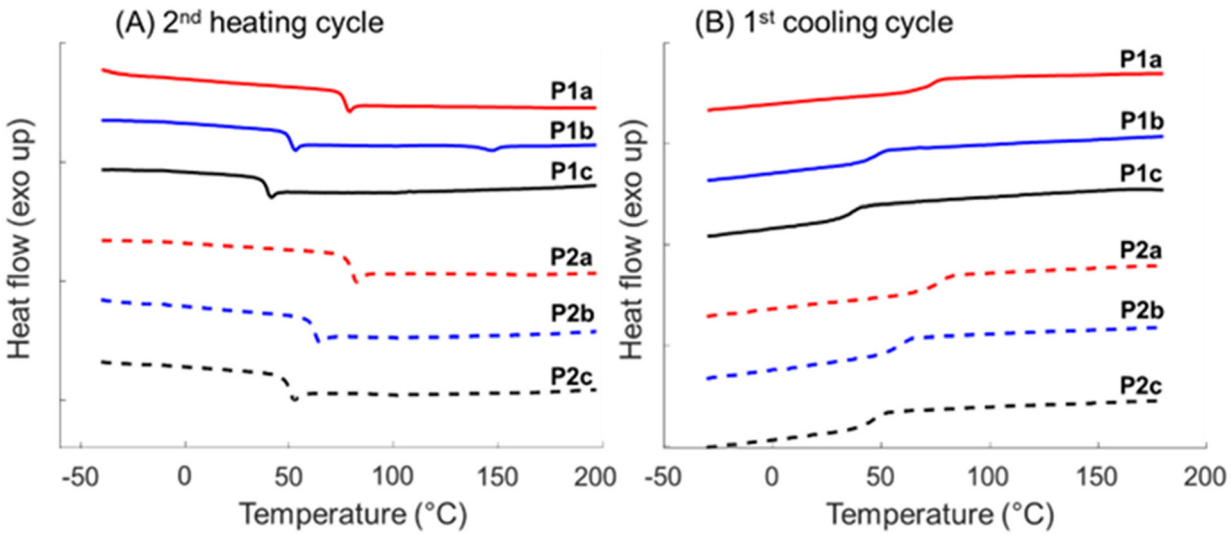

Fig. 2 DSC (A) 2nd heating and (B) 1st cooling cycle of **P1a–c** and **P2a–c**.

commercial polyesters used in packaging, such as PET, PLA, and PETG, and slightly higher than other biobased polyesters with spirocyclic acetal units reported in the literature.[54–57] Furthermore, the T_g values for **P2a–c** were higher compared to that of the corresponding member in the **P1a–c** series (by 4–12 °C). This indicated that the additional methoxy groups in **P2a–c** increased the bulkiness and reduced the segmental mobility of the backbones, which was consistent with other reported polymers with methoxy side groups.[58,59] The glass transition of all these polymers was also observed in the 1st cooling curves (Fig. 2B).

Because **P1b** showed slow crystallization in the DSC measurements, all the polymers were thermally annealed (during the second cooling cycle) at a temperature that was 20 °C above their respective T_g for 3 h. Afterward, the samples were cooled to −50 °C to start the third heating cycle (Fig. 3).

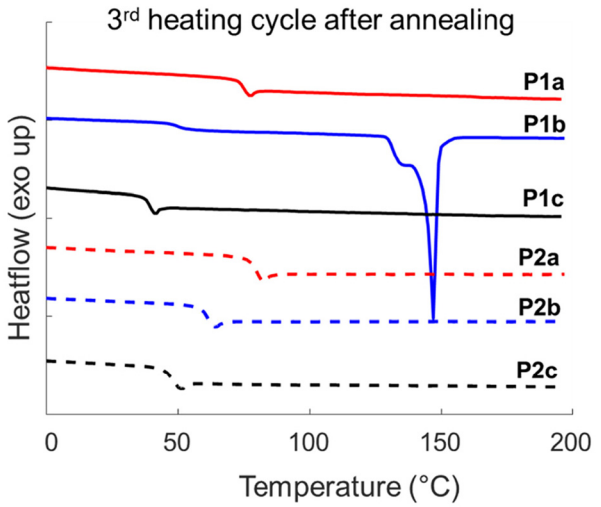

Fig. 3 DSC third heating cycle of polyesters after thermal annealing for 3 h during the second cooling cycle (curves not shown).

Consequently, the melting endotherm of **P1b** was notably larger during the third heating cycle, indicating a significant increase in crystallinity due to the thermal annealing process. However, all the other polymers remained completely amorphous after annealing (Fig. 3). The reason for the unique crystallization behavior of **P1b** remains to be explored, but it may be related to the absence of a methoxy group in **P1b** (compared to **P2a–c**) which increases the regularity and packing of the chains. In addition, it also has relatively low molecular weight among the series (compared to **P1a** and **P1c**), which can increase the crystallization rate.[60,61]

Thermomechanical properties

The thermomechanical properties of the polyesters were analyzed by DMA (Fig. 4). The samples were subjected to an oscillatory deformation while heated from room temperature to 100 °C with a rate of 3 °C min^{-1}. As a result, the storage moduli (E') of all the samples exhibited a characteristic 2 orders of magnitude reduction, followed by a rubber plateau (Fig. 4A). The E' was in the range of 1–3 GPa at the glassy plateau (at 30 °C), which was comparable to that of commercial polyesters like PET and PLA.[48,62–64] The E' curves for **P2b** and **P2c** showed a slight increasing trend after the glass transition, which might be due to cold crystallization.[65–67] The T_g values (taken from E'' data as the temperature at the peak value, Fig. 4B and Table 2) also showed a decreasing trend with increased length of the alkylene units, which is consistent with the DSC results (Table 1). The slightly different T_g values according to DMA and DSC results were due to the differences in the mechanical and thermal response in connection with the glass transition, which is a commonly observed effect.[68]

Acidic hydrolysis

Two polyesters from each series (**P1a** and **P2a**) were selected for a preliminary investigation of their chemical recyclability under acidic conditions. The polymer powders were suspended in concentrated HCl (12 M) and stirred at 70 °C for 24 h while

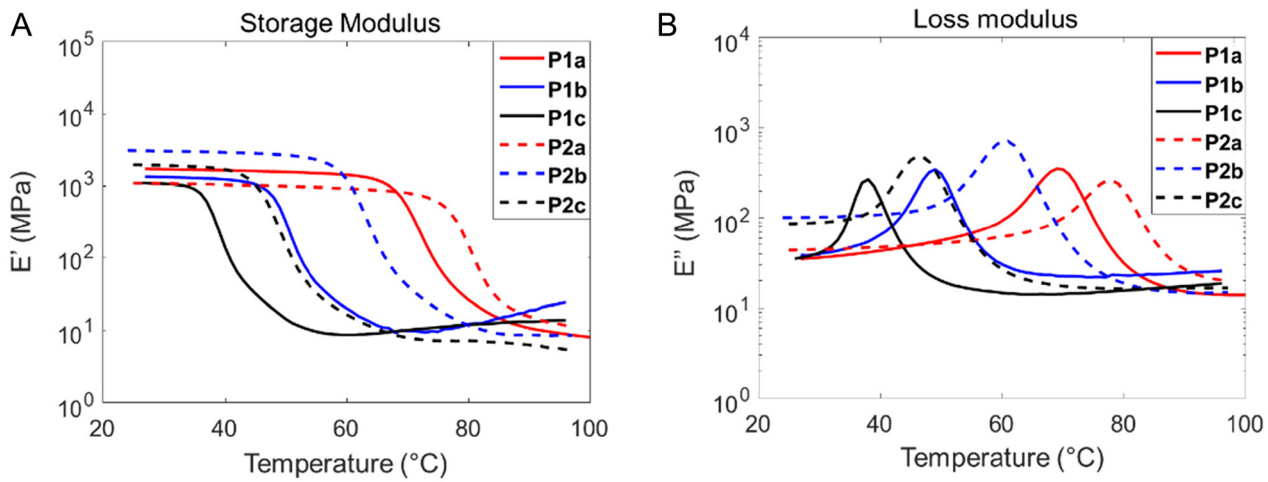

Fig. 4 DMA temperature sweep showing the (A) storage moduli, E', and (B) loss moluli, E'' of the obtained polyesters.

Table 2 DMA results of the obtained polyesters

Polymer	T_g [a] (°C)	T_g [b] (°C)	E' [c] (MPa)
P1a	69	79	1720
P1b	49	53	1340
P1c	38	41	1070
P2a	78	83	1100
P2b	60	65	3080
P2c	46	52	1930

[a] T_g was measured as the peak temperatures in the E'' curves. [b] T_g was measured by DSC. [c] E' was measured as the storage modulus at the glassy plateau at 30 °C for the polyesters.

being constantly monitored by visual inspection (Fig. 5). For both samples, the initial polymer powders gradually turned into finer particles, which formed a heterogeneous slurry after 24 h (Fig. S33, ESI†). Interestingly, the **P1a** slurry remained white throughout the hydrolysis experiment, while the **P2a** slurry turned brown after 8 h, and then black after 24 h. The coloration during the hydrolysis of **P2a** was consistent with side reactions commonly observed when working with lignin and the formation of humic substances.[69–72]

After the hydrolysis, the slurry was diluted with water, and the pH was adjusted to ~1 by the addition of K_2CO_3 powder. The resulting slurry was then filtered, and the aqueous phase was extracted with DCM. The filtered crude solid and the concentrated organic phase were both analyzed by ^{1}H NMR spectroscopy (Fig. S34 and 35†). In the case of **P1a**, the solid was identified as a bisphenol **BP1** (Fig. 5), with 71% yield and relatively high purity according to the ^{1}H NMR spectrum (Fig. S34B, ESI†). This recovered **BP1** structure has been previously investigated in the production of liquid crystalline polyesters,[73] and it could act as a potential monomer for other polymers like polycarbonates, polyesters, or polyurethanes. In addition, this bisphenol may also have potential in biomedical applications.[74] However, direct repolymerization (*i.e.* polyacetalization) of the obtained **BP1** with dibromomethane was not possible, due to incomplete conversion of the phenol groups (Fig. S36, ESI†). The filtrate (from the organic phase) contained only negligible amounts (~2%) of dry substances, which were presumably small molecules formed by the hydrolysis of ester bond according to the ^{1}H NMR spectrum (Fig. S34C, ESI†). This indicated that the acidic hydrolysis mainly took place at the acetal bonds while the ester bonds remained largely intact under these conditions.

Acidic hydrolysis of **P2a** under the same conditions led to significantly different results, despite the seemingly similar structures of the two polymers (only the presence/absence of methoxy groups). After the hydrolysis of **P2a**, a black insoluble solid was isolated (in 21% yield), of which the structure could

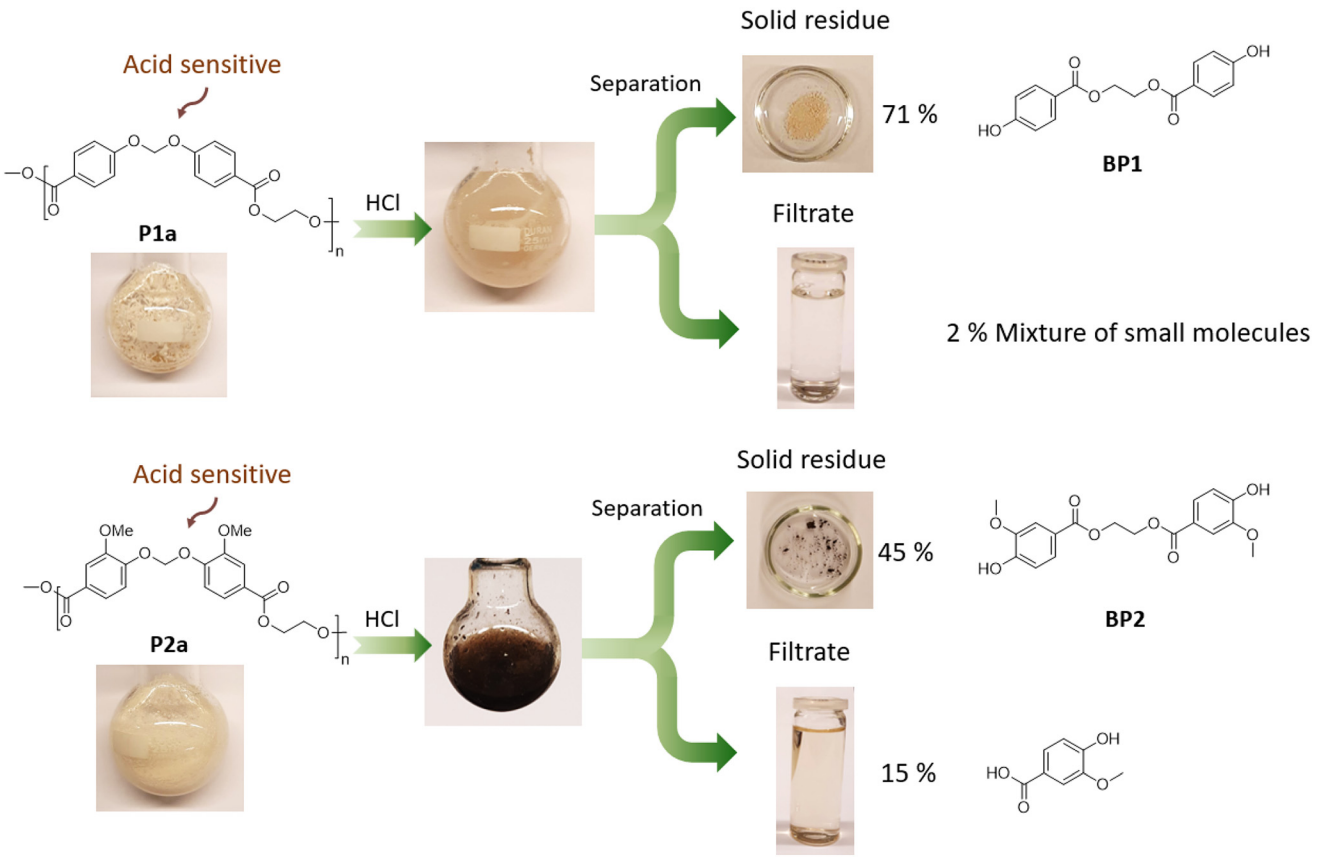

Fig. 5 Acidic hydrolysis of **P1a** and **P2a** in HCl (12.0 and 10.5 M, respectively), yielding a solid residue and a liquid filtrate phase after filtration.

not be identified. In the meantime, vanillic acid was recovered (in 31% yield) from the organic phase (Fig. S35, ESI†). This indicated that both the acetal and ester bonds in **P2a** were hydrolyzed. To explore the possibility to gain better control over the hydrolysis process and achieve selective hydrolysis of the acetal bonds in **P2a**, different experimental conditions were investigated (Table S3 and Fig. S37–47, ESI†). The best result was observed when 10.5 M of HCl was used at 70 °C. Under this condition, the corresponding bis-phenol (**BP2**) was recovered in 45% yield as a solid residue. However, we also observed 15% of vanillic acid in the organic phase, which indicated that some ester bonds were still hydrolyzed. The use of even lower concentrations of HCl (3–9 M), or milder organic acids (formic acid and oxalic acid) did not result in any significant hydrolysis, and the polymer remained intact as the solid residue (Fig. S45–47, ESI†).

According to our observations, the hydrolysis of **P2a** was significantly faster than that of **P1a**, which indicated the effect of the methoxy groups in the *ortho* position to the acetal. To gain a further insight, a model hydrolysis of the two monomers (methyl paraben and methyl vanillate) was carried out in 12 M HCl at 70 °C for 4 h, which was basically ester hydrolysis. The production of carboxylic acids (*i.e.*, 4-hydroxylbenzoic acid and vanillic acid, respectively) and the mass of the residual solid weight were monitored (Fig. S48–49, eqn (S2)–(S5), ESI†). As a result, the consumption of methyl vanillate and formation of vanillic acid was both faster than that of methyl paraben and 4-hydroxylbenzoic acid, which indicated that the presence of methoxy groups could enhance the acidic hydrolysis of the ester bonds. Although the exact reason remained to be explored, the enhanced hydrolysis rate by the presence of methoxy group could be related to the electron donating effect of methoxy group.[75] In principle, the methoxy group can stabilize the positively charged transition state,[34] which will thus facilitate the hydrolysis. However, other factors such as steric hindrance (by the methoxy groups) and the acidity of the leaving group may also play a role. In the literature, decreased thermal stability of molecules and polymers by the presence of methoxy groups have also been reported.[76–78]

We also noticed that there was no color change during the acidic hydrolysis of both monomers. However, the solution obtained from the hydrolysis of methyl vanillate turned black after the addition of one drop of formaldehyde (Fig. S49, ESI†). This observation suggested that the color change during the hydrolysis of **P2a** could be attributed to formaldehyde-related side reactions. To gain a further insight, a model reaction was carried out by reacting formaldehyde and vanillic acid (equimolar amounts in 12 M HCl) at 70 °C until it started to turn dark (*ca.* 2 h). Afterwards, a pale-yellow solid residue and dark-brown concentrated filtrate were obtained using the same separation procedure adopted for the hydrolysis of **P2a**. ^{1}H-NMR analysis revealed that the solid residue consisted of vanillic acid (Fig. S51, ESI†), whereas the concentrated filtrate presented the expected peaks for vanillic acid, but also a series of peaks at 3.8–3.9, 4.2–5.5, 6.5–8.0 and 9.3–10.4 ppm that could not be elucidated. Some of these peaks (*e.g.* those observed at 5.2, 7.2–7.4 and 9.4–9.9 ppm) were also present in the spectra of the analogous filtrate obtained from the acidic hydrolysis of **P2a** in HCl 12 M (Fig. S35 and S51, ESI†), indicating that the black coloration observed during the acidic hydrolysis of **P2a** could be related to the side reactions involving vanillic acid and formaldehyde (which could form during the hydrolysis of the acetal bonds).

Conclusions

Two series of novel biobased poly(acetal-ester)s with non-cyclic acetal units, tunable T_gs, and reasonably high molecular weights were synthesized, which provided an insight into the fundamental structure–property relationship of this new class of polymers. The key parameters for the monomer synthesis were evaluated according to their GHG emissions, which provided a preliminary environmental insight for the further development of such polymers in the future. Furthermore, the non-cyclic acetals in this class of polymers could be selectively cleaved under acidic hydrolysis conditions, which could facilitate chemical recycling by the molecular design. We also observed that the presence of methoxy groups on the polymer backbone accelerated the hydrolysis, which could enable hydrolysis under milder conditions. However, this also increased the risk of coloration due to side reactions. The nature of the coloration and side reaction was preliminarily investigated by model reactions of the corresponding small molecules. In general, this work provided an effective method to design and fabricate recyclable polyesters by utilizing biosourced (*e.g.* lignin-based) monomeric hydroxybenzoic acids with or without methoxy groups. In the future, synthetic investigations of more structural varieties (*e.g.* the substitution on the acetal carbon, or other substitutions on the phenolic rings) are expected to provide deeper knowledge about how to utilize non-cyclic acetals in the design of chemically recyclable biobased polymers.

Data availability

The data supporting this article have been included as part of the ESI.†

Conflicts of interest

There are no conflicts to declare.

Acknowledgements

This work was financially supported by the Mistra Foundation (the "STEPS" project, No. 2016/1489), Swedish Research Council for Sustainable Development (Formas, No. 2021-01107), Carl-Trygger Foundation (No. 18:435), the Crafoord Foundation (No. 20160774 and 20180939), and the Royal

Physiographic Society in Lund. We thank John P. Jensen from Nordzucker Technology for valuable discussions, Sofia Essén for the mass spectrometry measurements.

References

1 R. Geyer, J. R. Jambeck and K. L. Law, *Sci. Adv.*, 2017, **3**, e1700782.
2 S. A. Park, H. Jeon, H. Kim, S. H. Shin, S. Choy, D. S. Hwang, J. M. Koo, J. Jegal, S. Y. Hwang, J. Park and D. X. Oh, *Nat. Commun.*, 2019, **10**, 2601.
3 J. G. Rosenboom, D. K. Hohl, P. Fleckenstein, G. Storti and M. Morbidelli, *Nat. Commun.*, 2018, **9**, 2701.
4 O. Hauenstein, S. Agarwal and A. Greiner, *Nat. Commun.*, 2016, **7**, 1–7.
5 R. Hatti-Kaul, L. J. Nilsson, B. Zhang, N. Rehnberg and S. Lundmark, *Trends Biotechnol.*, 2020, **38**, 50–67.
6 J. G. Rosenboom, R. Langer and G. Traverso, *Nat. Rev. Mater.*, 2022, **7**, 117–137.
7 T. P. Kainulainen, T. I. Hukka, H. D. Özeren, J. A. Sirviö, M. S. Hedenqvist and J. P. Heiskanen, *Biomacromolecules*, 2020, **21**, 743–752.
8 C. Pang, J. Zhang, Q. Zhang, G. Wu, Y. Wang and J. Ma, *Polym. Chem.*, 2015, **6**, 797–804.
9 S. Subramaniyan, N. Najjarzadeh, S. R. Vanga, A. Liguori, P. O. Syrén and M. Hakkarainen, *ACS Sustainable Chem. Eng.*, 2023, **11**, 3451–3465.
10 M. Moroni and A. Mei, *Appl. Sci.*, 2020, **10**, 2800–2818.
11 P. R. Christensen, A. M. Scheuermann, K. E. Loeffler and B. A. Helms, *Nat. Chem.*, 2019, **11**, 442–448.
12 A. R. Rahimi and J. M. Garciá, *Nat. Rev. Chem.*, 2017, **1**, 1–11.
13 Z. Guo, M. Eriksson, H. de la Motte and E. Adolfsson, *J. Cleaner Prod.*, 2020, 124579.
14 S. Thiyagarajan, E. Maaskant-Reilink, T. A. Ewing, M. K. Julsing and J. Van Haveren, *RSC Adv.*, 2022, **12**, 947–970.
15 N. Warlin, E. Nilsson, Z. Guo, S. V. Mankar, N. G. Valsange, N. Rehnberg, S. Lundmark, P. Jannasch and B. Zhang, *Polym. Chem.*, 2021, **12**, 4942–4953.
16 N. G. Valsange, R. N. L. de Menezes, N. Warlin, S. V. Mankar, N. Rehnberg, B. Zhang and P. Jannasch, *Macromolecules*, 2024, **57**, 2868–2878.
17 R. N. L. de Menezes, O. Gordivska, T. T. Nguyen, N. Warlin, N. Rehnberg and B. Zhang, *React. Funct. Polym.*, 2024, **205**, 106062.
18 N. Warlin, M. N. Garcia Gonzalez, R. Menezes, A. Karajos, E. Olsson, C. Almqvist, M. Sayed, S. V. Mankar, N. Valsange, O. Y. Abdelaziz, C. P. Hulteberg, F. G. Bäcklund, Z. Guo, N. Rehnberg, S. Lundmark, R. Hatti-Kaul, P. Jannasch and B. Zhang, *ChemSusChem*, 2024, e202402067.
19 S. V. Mankar, J. Wahlberg, N. Warlin, N. G. Valsange, N. Rehnberg, S. Lundmark, P. Jannasch and B. Zhang, *ACS Sustainable Chem. Eng.*, 2023, **11**, 5135–5146.
20 N. G. Valsange, N. Warlin, S. V. Mankar, N. Rehnberg, B. Zhang and P. Jannasch, *Green Chem.*, 2024, **26**, 2858–2873.
21 R. Sedrik, O. Bonjour, S. Laanesoo, I. Liblikas, T. Pehk, P. Jannasch and L. Vares, *Biomacromolecules*, 2022, **23**, 2685–2696.
22 N. G. Valsange, M. N. Garcia Gonzalez, N. Warlin, S. V. Mankar, N. Rehnberg, S. Lundmark, B. Zhang and P. Jannasch, *Green Chem.*, 2021, **23**, 5706–5723.
23 A. Hufendiek, S. Lingier and F. E. Du Prez, *Polym. Chem.*, 2019, **10**, 9–33.
24 K. Saito, F. Eisenreich and Ž. Tomović, *Macromolecules*, 2024, **57**, 8690–8697.
25 L. P. Manker, G. R. Dick, A. Demongeot, M. A. Hedou, C. Rayroud, T. Rambert, M. J. Jones, I. Sulaeva, M. Vieli, Y. Leterrier, A. Potthast, F. Maréchal, V. Michaud, H.-A. Klok and J. S. Luterbacher, *Nat. Chem.*, 2022, **14**, 976–984.
26 A. G. Pemba, M. Rostagno, T. A. Lee and S. A. Miller, *Polym. Chem.*, 2014, **5**, 3214–3221.
27 B. Kwon, E. Han, W. Yang, W. Cho, W. Yoo, J. Hwang, B. M. Kwon and D. Lee, *ACS Appl. Mater. Interfaces*, 2016, **8**, 5887–5897.
28 W. Yang, J. Noh, H. Park, S. Gwon, B. Singh, C. Song and D. Lee, *Biomaterials*, 2018, **154**, 48–59.
29 S. Park, B. Kwon, W. Yang, E. Han, W. Yoo and D. Lee, *J. Controlled Release*, 2014, **196**, 19–27.
30 S. Samanta, C. C. De Silva, P. Leophairatana and J. T. Koberstein, *J. Mater. Chem. B*, 2018, **6**, 666–674.
31 T. Hashimoto, H. Meiji, M. Urushisaki, T. Sakaguchi, K. Kawabe, C. Tsuchida and K. Kondo, *J. Polym. Sci., Part A: Polym. Chem.*, 2012, **50**, 3674–3681.
32 L. Zhao, L. Zhang and Z. Wang, *RSC Adv.*, 2015, **5**, 95126–95132.
33 Q. Li, S. Ma, S. Wang, Y. Liu, M. A. Taher, B. Wang, K. Huang, X. Xu, Y. Han and J. Zhu, *Macromolecules*, 2020, **53**, 1474–1485.
34 B. Liu and S. Thayumanavan, *J. Am. Chem. Soc.*, 2017, **139**, 2306–2317.
35 L. Zimmermann, A. Dombrowski, C. Völker and M. Wagner, *Environ. Int.*, 2020, **145**, 106066.
36 Z. Demchuk, N. Wu, G. Pourhashem and A. Voronov, *ACS Sustainable Chem. Eng.*, 2020, **8**, 12870–12876.
37 M. A. F. Delgove, A. B. Laurent, J. M. Woodley, S. M. A. De Wildeman, K. V. Bernaerts and Y. van der Meer, *ChemSusChem*, 2019, **12**, 1349–1360.
38 N. Warlin, M. N. Garcia Gonzalez, S. Mankar, N. G. Valsange, M. Sayed, S. H. Pyo, N. Rehnberg, S. Lundmark, R. Hatti-Kaul, P. Jannasch and B. Zhang, *Green Chem.*, 2019, **21**, 6667–6684.
39 S. V. Mankar, M. N. Garcia Gonzalez, N. Warlin, N. G. Valsange, N. Rehnberg, S. Lundmark, P. Jannasch and B. Zhang, *ACS Sustainable Chem. Eng.*, 2019, **7**, 19090–19103.
40 S. G. Yao, J. K. Mobley, J. Ralph, M. Crocker, S. Parkin, J. P. Selegue and M. S. Meier, *ACS Sustainable Chem. Eng.*, 2018, **6**, 5990–5998.
41 T. T. Nguyen, E. Olsson, S. V. Mankar, N. Warlin, N. G. Valsange, J. Engqvist, N. Rehnberg, P. Jannasch and B. Zhang, *Macromolecules*, 2024, **57**, 9289–9301.

42 J. O. Krömer, R. G. Ferreira, D. Petrides and N. Kohlheb, *Front. Bioeng. Biotechnol.*, 2020, **8**, 403.
43 I. S. Modahl and E. Soldal, *The 2019 LCA of products from Borregaard*, Sarpsborg, 2019.
44 Adesso Advanced Materials Wuxi Co., Ltd, WO2016177305A1, 2016.
45 P. Wang, C. R. Arza and B. Zhang, *Polym. Chem.*, 2018, **9**, 4706–4710.
46 X. Li, X. Wang, S. Subramaniyan, Y. Liu, J. Rao and B. Zhang, *Biomacromolecules*, 2022, **23**, 150–162.
47 H. Köpnick, M. Schmidt, W. Brügging, J. Rüter and W. Kaminsky, *Polyesters*, Wiley-VCH Verlag GmbH & Co. KGaA, Weinheim, Germany, 2000.
48 O. Y. Abdelaziz, M. B. Vives, S. V. Mankar, N. Warlin, T. T. Nguyen, B. Zhang, C. P. Hulteberg and A. Khataee, *iScience*, 2024, **27**, 109418.
49 C. R. Arza and B. Zhang, *ACS Omega*, 2019, **4**, 15012–15021.
50 F. Samperi, C. Puglisi, R. Alicata and G. Montaudo, *Polym. Degrad. Stab.*, 2004, **83**, 11–17.
51 H. Ohtani, T. Kimura and S. Tsuge, *Anal. Sci.*, 1986, **2**, 179–182.
52 P. Wang, J. A. Linares-Pastén and B. Zhang, *Biomacromolecules*, 2020, **21**, 1078–1090.
53 P. Wang and B. Zhang, *RSC Adv.*, 2021, **11**, 16480–16489.
54 N. G. Valsange, N. Warlin, S. V. Mankar, N. Rehnberg, B. Zhang and P. Jannasch, *Green Chem.*, 2024, **26**, 2858–2873.
55 N. Warlin, M. N. Garcia Gonzalez, S. Mankar, N. G. Valsange, M. Sayed, S.-H. Pyo, N. Rehnberg, S. Lundmark, R. Hatti-Kaul, P. Jannasch and B. Zhang, *Green Chem.*, 2019, **21**, 6667–6684.
56 S. V. Mankar, J. Wahlberg, N. Warlin, N. G. Valsange, N. Rehnberg, S. Lundmark, P. Jannasch and B. Zhang, *ACS Sustainable Chem. Eng.*, 2023, **11**, 5135–5146.
57 Omnexus, Glass Transition Temperature, **https://omnexus.specialchem.com/polymer-property/glass-transition-temperature**, (accessed 20 January 2025).
58 O. Bonjour, H. Nederstedt, M. V. Arcos-Hernandez, S. Laanesoo, L. Vares and P. Jannasch, *ACS Sustainable Chem. Eng.*, 2021, **9**, 16874–16880.
59 J. A. Emerson, N. T. Garabedian, D. L. Burris, E. M. Furst and T. H. Epps, *ACS Sustainable Chem. Eng.*, 2018, **6**, 6856–6866.
60 X. Chen, G. Hou, Y. Chen, K. Yang, Y. Dong and H. Zhou, *Polym. Test.*, 2007, **26**, 144–153.
61 J. R. Fried, *Polymer Science and Technology*, Prentice Hall, Westford, 3rd edn, 2014.
62 C. W. Chen, P. H. Liu, F. J. Lin, C. J. Cho, L. Y. Wang, H. I. Mao, Y. C. Chiu, S. H. Chang, S. P. Rwei and C. C. Kuo, *J. Polym. Environ.*, 2020, **28**, 2880–2892.
63 B. A. Alshammari, M. Hossain, A. M. Alenad, A. G. Alharbi and B. M. Alotaibi, *Polymers*, 2022, **14**, 1–14.
64 X. Wang, S. Peng, H. Chen, X. Yu and X. Zhao, *Composites, Part B*, 2019, **173**, 107028.
65 F. Ali, Y. W. Chang, S. C. Kang and J. Y. Yoon, *Polym. Bull.*, 2009, **62**, 91–98.
66 J. S. Lee, G. H. Hwang, Y. S. Kwon and Y. G. Jeong, *Polymer*, 2020, **202**, 122677.
67 M. Cristea, D. Ionita and M. M. Iftime, *Materials*, 2020, **13**, 1–24.
68 K. Whitcomb, Measurement of Glass Transition Temperatures by Dynamic Mechanical Analysis and Rheology, **https://www.tainstruments.com/applications-notes/measurement-of-glass-transition-temperatures-by-dynamic-mechanical-analysis-and-rheology/**, (accessed 20 January 2025).
69 J. P. Martin and K. Haider, *Soil Sci. Soc. Am. J.*, 1976, **40**, 377–380.
70 S. Tang, F. Li, N. T. Tsona, C. Lu, X. Wang and L. Du, *ACS Earth Space Chem.*, 2020, **4**, 862–872.
71 Y. Zhang and M. Naebe, *ACS Sustainable Chem. Eng.*, 2021, **9**, 1427–1442.
72 A. Burges, H. M. Hurst, S. B. Walkden, F. M. Dean and M. Hirst, *Nature*, 1963, **199**, 696–697.
73 J. A. Moli, S. Vasanthi, N. Prakash and D. R. Singh, *High Perform. Polym.*, 2012, **24**, 507–520.
74 Rutgers, The State University of New Jersey, US10087285B2, 2018.
75 I. Meloche and K. J. Jaidler, *J. Am. Chem. Soc.*, 1951, **73**, 1712–1714.
76 M. Hasegawa, Y. Tsujimura, K. Koseki and T. Miyazaki, *Polym. J.*, 2008, **40**, 56–67.
77 C. R. Arza, P. Wang, J. Linares-Pastén and B. Zhang, *J. Polym. Sci., Part A: Polym. Chem.*, 2019, **57**, 2314–2323.
78 B. G. Harvey, A. J. Guenthner, W. W. Lai, H. A. Meylemans, M. C. Davis, L. R. Cambrea, J. T. Reams and K. R. Lamison, *Macromolecules*, 2015, **48**, 3173–3179.